Calorimetric Investigation of the Antiferromagnetic Transition in $NiCl_2 \cdot 6H_2O$[†]

W. L. Johnson* and W. Reese

Naval Postgraduate School, Monterey, California 93940

(Received 13 March 1970)

Measurements of the heat capacity of $NiCl_2 \cdot 6H_2O$ were made in the vicinity of the antiferromagnetic transition using calorimetric techniques of sufficient resolution so that the observed behavior was intrinsic to the samples studied. Two crystals of different origins were investigated in zero field, and one crystal was investigated with external fields applied parallel to the easy axis. The temperature of the heat-capacity maximum T_{max} differed by approximately 3 mK between the two crystals, but the heat-capacity anomalies of each were best described with the same value of T_N, 5.348 K. This value of T_N was 9 and 12 mK above the temperatures at which the maximum heat capacity occurred. The data implied critical exponents of 0.20 ± 0.03 above the transition and 0.00 ± 0.01 below. An analysis of the data in terms of the imaginary temperature described the rounding of the calorimetric anomaly which occurred below T_{max}. The analysis yielded best values for the imaginary part of the temperature comparable to the shift between T_N and T_{max}. The application of an external field caused a slow monotonic decrease in the amplitude and an increase in the width of the calorimetric anomaly. The width could be described by $\Delta^2 = \Delta_0{}^2 + aH$, suggesting that the broadening of the transition could be described by two independent mechanisms, one intrinsic to the sample and the second field dependent. The shift of the T_{max} with field was proportional to H^2.

INTRODUCTION

The antiferromagnet nickel chloride hexahydrate has been the subject of numerous investigations. Included in these was a determination of the specific heat in zero applied magnetic field from 1.4 to 20 K.[1] This study showed that the transition displayed the familiar "λ-shaped" anomaly with the peak heat capacity occurring near 5.34 K. Temperature resolution in this study was insufficient to determine the behavior near the transition with any confidence. Because of the current interest in the behavior of thermodynamic properties near phase transitions, a reexamination of the calorimetric transition in $NiCl_2 \cdot 6H_2O$, with and without applied magnetic fields, was undertaken using calorimetric techniques of sufficient resolution so that the behavior exhibited by the specific heat was intrinsic to the samples investigated rather than an artifact of the techniques employed.

The observed heat-capacity anomaly showed considerable "rounding," the extent of which differed slightly between the two crystals investigated. Analysis of the data showed that the best analytic description was obtained with a logarithmic divergence at temperatures lower than the transition and with a power-law divergence at higher temperatures. In the power-law region the best exponent was approximately 0.20. A feature of the analysis was that the temperature on which the divergence appeared to center, here called T_N, differed considerably (up to 12 mK) from the temperature at which the heat capacity was maximum T_{max}. When the rounding was investigated using the complex

temperature concept the best value for the imaginary part of the temperature was found to be quite comparable with the difference between T_N and T_{max}. A similar feature of the transition in non-ideal Ising-model systems has recently been discussed by Fisher and Ferdinand.[2,3] Application of a magnetic field parallel to the easy axis lowered the transition temperature in a manner consistent with the expected H^2 dependence. In addition to shifting the temperature of the heat-capacity peak, the presence of an applied field was found to slightly broaden the calorimetric anomaly. The empirical relationship $\Delta^2 = \Delta_0^2 + aH$ was found to describe this phenomenon, although other descriptions could also fit the data satisfactorily. Here Δ is a measure of the width of the calorimetric anomaly.

A brief summary of the known properties of $NiCl_2 \cdot 6H_2O$ is as follows. The crystal is monoclinic, of space group $C2/m$.[4] Each Ni ion is surrounded by a bi-prism consisting of two Cl ions and four waters of hydration. These units are joined by hydrogen bonds to form two-dimensional layers in the a-b plane. These layers are joined by weaker hydrogen bonds in the c direction. It is not known if the exchange linkages reflect this predominantly two-dimensional structure. Measurements of the susceptibility of single-crystal samples[5,6] show that the susceptibility measured perpendicular to the c axis decreases below approximately 6 K, whereas below this temperature the susceptibility perpendicular to the other two axes is nearly temperature independent. Above 6 K, the susceptibility is nearly isotropic with a g factor of

2. 2 and a Wiess temperature of 10 K. The results of antiferromagnetic-resonance[7] and neutron scattering[8] studies show that the sublattice magnetization lies in the a-c plane, inclined about 10° from the a axis toward the c axis. The effective exchange field was found to be 86 kOe, much larger than the anisotropy fields, by means of the antiferromagnetic-resonance studies.

EXPERIMENTAL DETAILS

The measurements were taken over the temperature range 4. 3 to 5. 9 K using an adiabatic calorimeter and the discontinuous heating method. The calorimeter employed a mechanical heat switch. The sample was supported by nylon threads from a copper C which was mounted by a pivot from the adiabatic shield. This allowed the sample to be oriented with respect to the magnetic field. The field was supplied by a superconducting solenoid. The cryostat provided for two separate helium baths: an outer bath maintained at 4. 2 K in which the solenoid was placed and an inner bath which could be pumped, if desired. This latter feature was not employed in these experiments. Complete details of the cryostat design are presented elsewhere. [9]

Two thermometers, both mounted on the sample, were employed in this experiment. A gold-doped germanium resistor served as a transfer standard while a carbon radio resistor with a nominal 470-Ω value served as the primary temperature sensor. The carbon thermometer was so employed because the change in its resistance due to the application of magnetic fields was much smaller than the corresponding change for the germanium resistor. The correction for magnetoresistance in the carbon thermometer was checked at 4. 2 K and extrapolated into the range in which measurements were conducted using standard formulas from the literature. [10,11] The germanium thermometer was calibrated using a gas-bulb thermometer and the calibration was checked by measurement of the heat capacity of copper. Over the temperature range 4 to 20 K, these copper measurements differed by no more than 0. 5% from the values predicted by the copper reference formula. [12] Based on this comparison it is estimated that the temperature scale employed in this work has an accuracy of better than 0. 5%. The carbon thermometer was calibrated against the germanium thermometer in zero field at times when there was no distinguishable drift of the thermometer temperature. The resistance of the thermometers was determined using a 37-Hz Wheatstone bridge which dissipated less than 10 nW of power while the measurements were performed. The temperature could be determined with a precision of 1 μK. In this work a

minimum step of 0. 7 mK was used, although smaller steps could have been employed if the sharpness of the transition had demanded it. The accuracy with which determinations of the heat capacity could be made in the vicinity of the calorimetric peak was approximately 0. 3%.

Two single-crystal samples were employed in these studies. One crystal, labeled K-2, was obtained from R. L. Kleinberg and has a mass of 0. 1 g. The second, labeled J-1, was grown from reagent-grade salt by evaporation from aqueous solution and had a mass of 0. 72 g during the measurements. The crystal axes were identified from the crystal habit[13] and this assignment was tested using the known cleavage properties associated with the predominantly two-dimensional structure. As $NiCl_2 \cdot 6H_2O$ can both absorb water from the atmosphere and lose waters of hydration when exposed to vacuum, the crystal was protected as well as possible by coating with Krylon spray and then dipping in GE 7031 varnish as early in the mounting procedure as was possible. This protection was not perfect; as an example, crystal J-1 lost 0. 04 g during sample preparation and mounting.

In addition to the thermometers, the Krylon coating, and the nylon supporting threads, the addenda consisted of 0. 033 g of GE 7031 varnish, a 100-Ω manganin heater, and a bare copper wire which served as the thermal link to the heat switch. Because of the small heat capacity of the addenda, the determination of the addenda heat capacity by direct measurement was not feasible. Thus, the contribution of the addenda to the total heat capacity was estimated from published data. The addenda heat capacity represented a small contribution to the total, never more than 2%, and only 0. 3% in the vicinity of the heat-capacity maximum.

RESULTS IN ZERO FIELD

The results[14] obtained in zero applied field are shown in Fig. 1(a). For this presentation of the data, the same lattice subtraction as was made by Robinson and Friedberg[1] has been effected so that the data should represent the magnetic contribution to the specific heat, C_M. It is apparent that the present data agree quite well with the previous results, except in the immediate vicinity of the calorimetric peak. Figure 1(b) displays the data on a more expanded temperature scale. A considerable rounding of the peak is obvious from this presentation as are differences between the results obtained in the immediate vicinity of the peak for the two crystals investigated. The calorimetric peak observed in crystal K-2 is sharper and higher than that observed in crystal J-1 and occurs 3 mK higher in temperature.
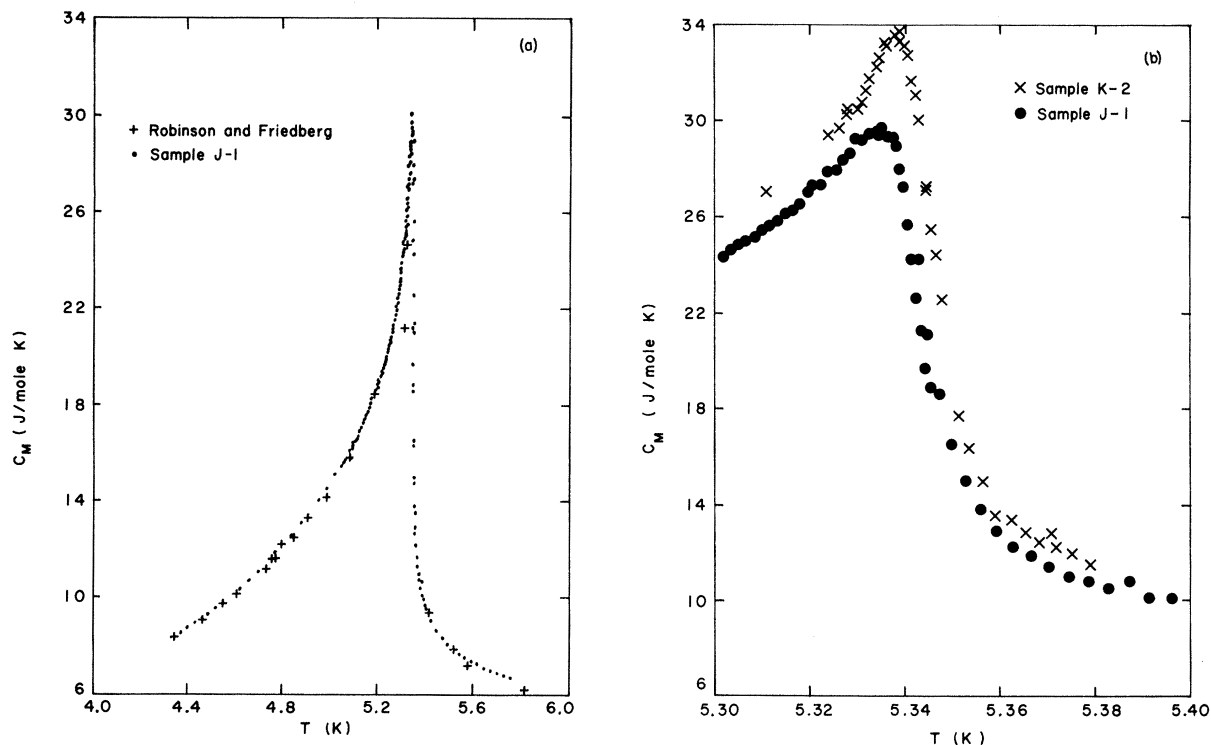
FIG. 1. (a) Comparison of the magnetic portion of the heat capacity of $NiCl_2 \cdot 6H_2O$ as determined by Robinson and Friedberg and in the present experiment with crystal J-1; (b) higher-resolution presentation of C_M in zero field showing the differences observed between crystals J-1 and K-2.

To make contact with the current discussions of critical-point phenomena, it is necessary to attempt a functional fit to best describe the calorimetric anomaly. The presence of the observed rounding makes such a determination less than straightforward. The most important problem comes in the proper assignment of "transition temperature" T_N. A subsidiary problem appears when dividing the data into three regions: the region which is too far from the transition to represent critical behavior, the critical region, and the region dominated by rounding. As far as this latter problem is concerned it was observed that the critical parameters obtained in the analysis were quite insensitive to readjustments of the boundaries between the three regions. Thus, although the boundaries are hazy, the choices made for them had scant influence on the outcome of the analysis. A preliminary step in the analysis is shown in Fig. 2(a) where C_M is plotted against $\log_{10} |1 - T/T_{max}|$. This presentation displays the marked difference in behavior observed above and below T_{max} and allows a preliminary assignment of the rounded region, which extends to approximately $|1 - T/T_{max}| \approx 10^{-3}$ for crystal J - 1, the crystal for which the data are shown in Fig. 2(a).

The next step is to fit C_M to the suggested forms

$$C = (A/\alpha)[(\epsilon^{-\alpha} - 1)] + B, \quad T > T_N$$

$$C = (A'/\alpha')(\epsilon^{-\alpha'} - 1) + B', \quad T < T_N$$

where $\epsilon = |1 - T/T_N|$. For $\alpha = 0$, a logarithmic fit is used. The parameters A, A', B, B', α, α', and T_N are treated as adjustable and the data above and below T_{max} fitted independently. The procedure adopted was that suggested by van der Hoeven et al. [15] and will be explained for the case $T > T_N$. Values for α and T_N are first assumed and a linear least-squares fit performed on that portion of the data set selected as lying in the critical region so as to choose values for A and B. The correlation coefficient $\gamma = (1 - \delta/N\sigma^2)^{1/2}$ (where δ is the sum of the square deviations between the fit and the data set, N is the number of points fitted, and σ is the variance) is computed. This procedure is repeated holding α constant and varying T_N. This gives γ as a function of T_N for the first value of α. The entire procedure is repeated for various values of α. The resulting family of curves, illustrated in Fig. 3, allows one to find the values of α and T_N (and hence A and B) which give the best representation of the data. An estimate of the un-
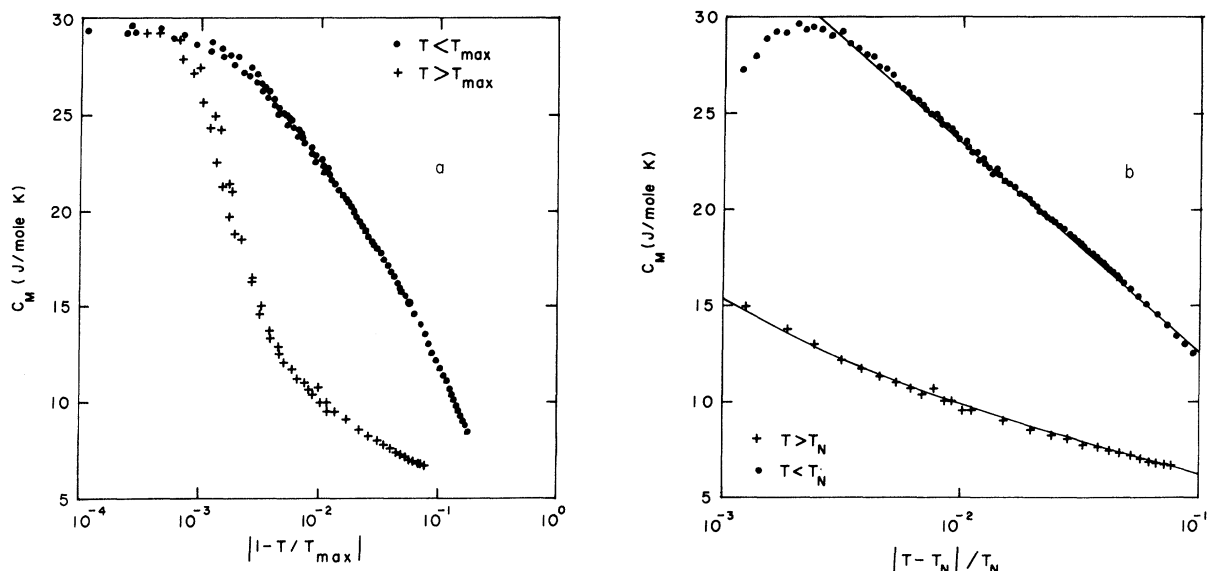
FIG. 2. (a) Semilogarithmic presentation of C_M for crystal J-1. This shows a preliminary stage in the data analysis, illustrates the approximate extent of the rounding of the heat-capacity peak, and illustrates the gross differences in behavior above and below T_{max}; (b) same data as is shown in (a) is here compared with the final fits, the parameters of which are shown in Table I; fits are shown by solid lines.
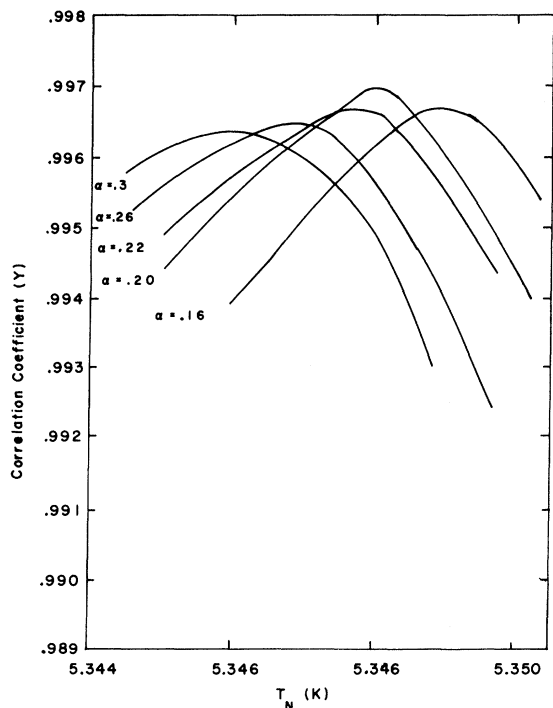

FIG. 3. Illustration of the method used to choose the critical exponent and T_N. Each curve gives the correlation coefficient for a linear least-squares fit to the data as a function of the temperature chosen as T_N for fixed values of α.

certainty in the critical parameters can be obtained by using best fits with parameters other than those which give maximum correlation and by observing when systematic deviations between the fitting formulas and the data become apparent. The results of this analysis procedure are given in Table I. An example of the fits obtained are shown in Fig. 2(b).

A notable feature of the analysis procedure was that a transition temperature considerably higher than T_{max} was indicated. Since approximately the same value of T_N was indicated for the analysis of each crystal and for the fits performed above and below T_N, despite the fact that T_{max} differed by 3 mK between the two crystals, there is some hope that this value of T_N represents the transition temperature of an "ideal" crystal of $NiCl_2 \cdot 6H_2O$.

A second feature of the analysis is that grossly different values of α and α' were obtained. This is similar to the result of several other careful studies of antiferromagnetic transitions. For example, in $MnCl_2 \cdot 4H_2O$, where rounding was less of a problem than in the present work, the results $\alpha = 0.35$ and $\alpha' = 0$ were obtained[16] and in MnF_2 the result $0 \leq \alpha < 1$ and $\alpha' = 0$ was obtained.[17] Differences between T_N and T_{max}, but not so extreme as those found here, have also been found previously in the analysis of calorimetric data in antiferromagnets.[18] It may well be noted that the values of α and α' obtained here are in remarkably close agreement with the values estimated for Ising mod-

TABLE I. Parameters used to best describe the calorimetric anomaly in two crystals of $NiCl_2 \cdot 6H_2O$. The second set of parameters for $T < T_N$ were computed treating T_N as fixed and utilizing the complex-temperature concept. γ is the correlation coefficient which described the fit.

		Crystal J-1	Crystal K-2
$T > T_N$			
	T_N	5.348 ± 0.001 K	5.348 ± 0.001 K
	α	0.17 ± 0.03	0.20 ± 0.03
	A	0.866 J/mole K	0.835 J/mole K
	B	3.9 J/mole K	3.9 J/mole K
	γ	0.998	0.997
$T < T_N$			
	T_N	5.3466 ± 0.001	5.3476 ± 0.001
	α'	0.00 ± 0.03	0.00 ± 0.01
	A'	4.6 J/mole K	5.15 J/mole K
	B'	2.2 J/mole K	1.86 J/mole K
	γ	0.9995	0.9999
	A'	4.14 J/mole K	3.91 J/mole K
	B'	3.6 J/mole K	6.07 J/mole K
	τ	10 ± 2 mK	5 ± 2 mK
	γ	0.9993	0.998
	$T_N - T_{max}$	12 mK	9 mK

el systems by Baker,[19] although it is unlikely that this model applies to nickel chloride hexahydrate. Further, we can not exclude the suggestion of Gaunt and Domb[20] that the true critical exponent will be obtained with $\epsilon < 10^{-4}$ below T_N and an apparent logarithmic dependence found outside that region due to a combination of terms in the expansion.

An attempt to extract additional information from the zero-field data was made by treating temperature as a complex quantity, $T^* = T + i\tau$. This procedure has been suggested by various considerations of Fisher[2,3,21] and has been used in the study of the effect of external fields on the ferromagnetic transition in EuS by Teaney *et al.*[22] In such a fit the data in the rounded region are included in the data set to be fit; and T_N the real part of the complex transition temperature is treated as fixed at the value determined by the previous analysis. A fitting procedure similar to that already described was carried out on the data with $T < T_{max}$ using α' and τ as adjustable. The same value of α' resulted as in the previous more conventional analysis which excluded the data lying the rounded region. The resulting fit is shown in Fig. 4 and compared with the conventional fit. The parameters of the second fit are given in Table I. Although success was obtained with this procedure for $T < T_{max}$, a notable lack of success was attained for $T > T_{max}$. Primarily, this took the form of a drift in the best value of α from that determined

in the previous analysis.

The best values of τ determined below T_{max} are quite comparable with the values of $T_N - T_{max}$ obtained previously. Such results have been discussed in connection with transitions in imperfect Ising systems by Ferdinand and Fisher.[3] In terms of these theoretical ideas both the shift of T_{max} from T_N and the rounding are due to the spatial limitation of correlations. In two-dimensional systems[2] it has been predicted that the shift should equal τ, but the conclusions regarding three-dimensional systems are less definite.

Another attempt to account for the rounding in a more conventional fashion was also made by assuming a Gaussian distribution of transition temperatures.[23] For this analysis the idealized behavior was taken to be that given by the first fit. This attempt was unsuccessful, since values of the half-width, which allowed $C(T_{max})$ to be matched, produced a much smaller displacement between T_N and T_{max} than observed. Thus, either the imaginary temperature analysis of the rounding
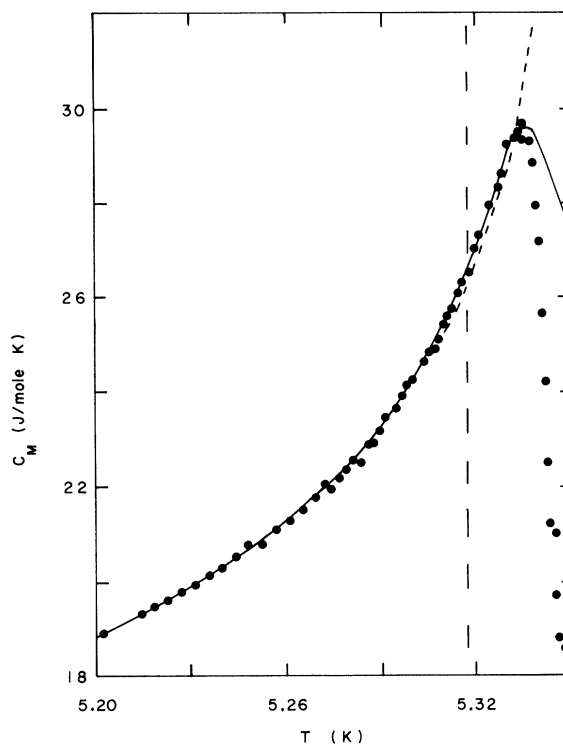

FIG. 4. Comparison of the best fit to the data below T_{max} using an undamped divergence and using the damped divergence produced when T is treated as complex. For the undamped fit, data falling to the right of the dashed line were discarded as "effected by the rounding." Some data lying at higher temperatures than T_{max} are also shown to aid in the location of T_{max}.

is to be preferred, or the shift between T_N and T_{max} obtained in the analysis of the present data is unrealistically large.

RESULTS IN APPLIED FIELDS

In addition to the measurements in zero field, calorimetric measurements were made on crystal K-2 in the temperature region near the peak of the calorimetric anomaly with magnetic fields to 19 kOe applied parallel to the easy axis. Fig. 5 displays the result of these measurements. The results can be summarized by stating that the application of the field shifts the transition to slightly lower temperatures and broadens the calorimetric peak slightly. Although the measurements do not extend over a sufficiently large range of temperatures to allow an accurate test of possible changes in the functional form of the calorimetric anomaly, no gross changes occurred. The curves, when plotted semilogarithmically, maintained the shape displayed by the zero-field data.

A quantitative investigation of the broadening of the transition caused by the application of the magnetic field is shown in Fig. 6. For this purpose Δ, the full width of the heat-capacity curve at 90% of $C(T_{max})$, is taken to characterize the width. This was done since $T_{max} \pm \Delta$ appears always to lie within the rounded region. The data are reasonably consistent with the form

$$\Delta^2 = \Delta_0^2 + aH,$$

with $a = 1.65 \times 10^{-8}$ K^2/Oe. This must be regarded purely as an empirical fit and slightly different

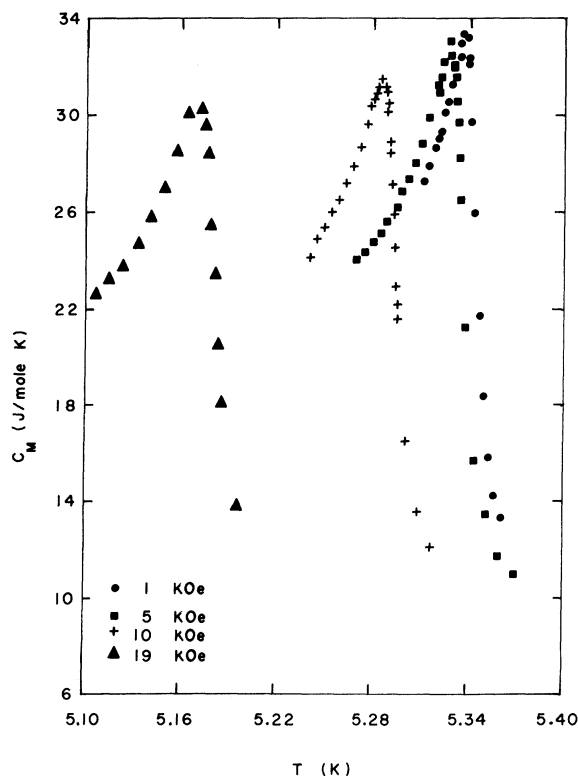FIG. 5. Heat capacity of NiCl$_2 \cdot$ 6H$_2$O in various applied fields as determined using crystal K-2.

forms, such as a linear relationship between Δ^2 and $H^{1/2}$, cannot be excluded. The data do definite-
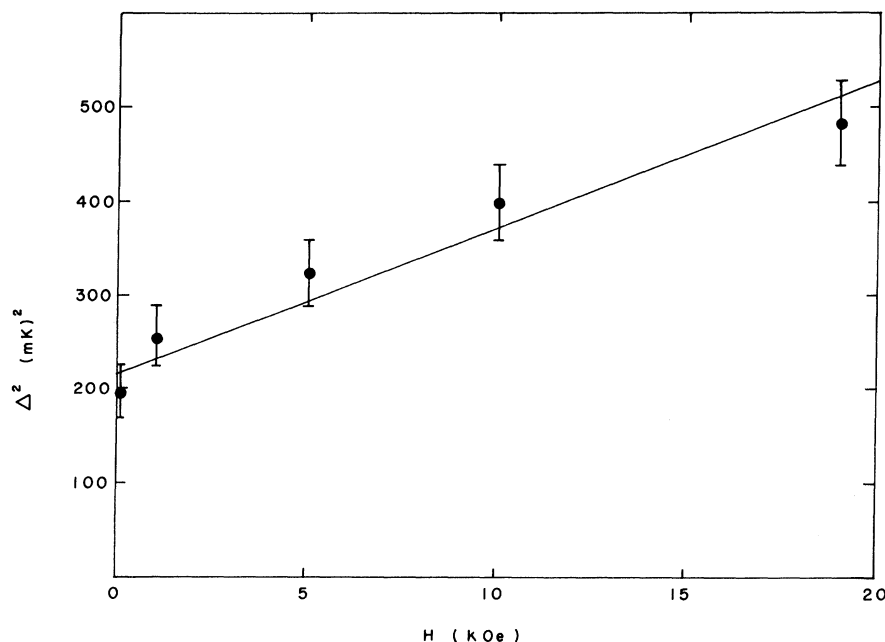

FIG. 6. Square of full width of the calorimetric anomaly at 90% of maximum Δ^2 is shown as a function of applied field for crystal K-2. Functional form suggested by the line drawn, $\Delta^2 = (2.2 \times 10^{-4} + 1.65 \times 10^{-8} H)$ K^2 is not uniquely determined by the data. However, the analysis suggests that the rounding is due to two independent causes, one intrinsic to the crystal and the second dependent on the field.
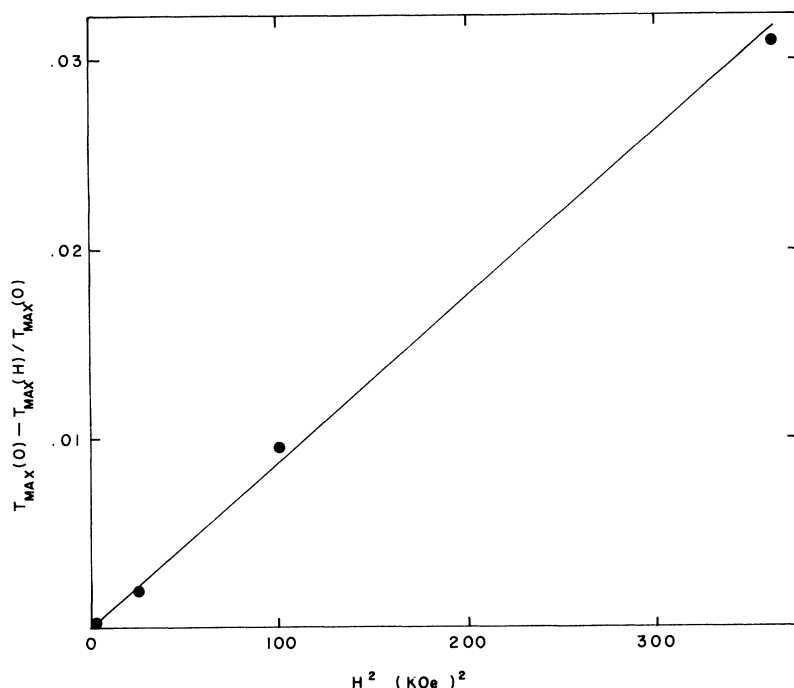
FIG. 7. Field-induced shift of the temperature of the calorimetric maximum is shown as a function of the square of the applied field. Field is applied along the easy axis. Line shows the fit

$$1 - T_{max}(H)/T_{max}(0) = 9 \times 10^{-11} \ Oe^{-2} H^2 \ .$$

ly indicate a relationship between Δ^2 and some simple function of H. This is suggestive of two independent broadening mechanisms, one intrinsic to the crystal and the second dependent on the applied field.

Both mean field theory[24] and the two-dimensional Ising model with superexchange[25] predict that the shift in the transition temperature will be proportional to H^2, although three-dimensional Ising models[26] seem to display a different dependence on H.

If we assume that the difference between T_{max} and T_N is nearly a constant, the data are reasonably consistent with a parabolic shift. This is shown in Fig. 7 in which $1 - T_{max}(H)/T_{max}(0)$ is plotted as a function of H^2. The slope of the line which fits the data, $9 \times 10^{-11} \ Oe^{-2}$, agrees only in order of magnitude with either the mean field or the two-dimensional Ising predictions when the appropriate constants to describe $NiCl_2 \cdot 6H_2O$ are used in the calculations.

---

†Work based on thesis submitted by W. L. J. in partial fulfillment of the requirements of the Ph. D degree.

*Present address: Department of Physics, University of Illinois, Urbana, Ill.

[1]W. K. Robinson and S. A. Friedberg, Phys. Rev. 117, 402 (1960).

[2]M. E. Fisher and A. E. Ferdinand, Phys. Rev. Letters 19, 169 (1967).

[3]A. E. Ferdinand and M. E. Fisher, Phys. Rev. 185, 832 (1969).

[4]J. Mizuno, J. Phys. Soc. Japan 16, 1574 (1961).

[5]T. Haseda, H. Kobayashi, and M. Date, J. Phys. Soc. Japan 14, 1724 (1959).

[6]R. B. Flippen and S. A. Friedberg, J. Appl. Phys. 31, 3385 (1960).

[7]M. Date and M. Motokawa, J. Phys. Soc. Japan 22, 165 (1967).

[8]R. Kleinberg, J. Appl. Phys. 38, 1453 (1967).

[9]W. L. Johnson, Ph. D thesis, Naval Postgraduate School, 1969 (unpublished).

[10]J. R. Clement and E. H. Quinnell, Rev. Sci. Instr. 23, 213 (1952).

[11]B. C. Belanger, Rev. Sci. Instr. 40, 1082 (1969).

[12]D. W. Osborne, H. E. Flotow, and F. Schreiner, Rev. Sci. Instr. 38, 159 (1967).

[13]P. Groth, Chemische Kristallographie (Wilhelm Engelman, Leipzig, 1906), I Teil, p. 247.

[14]A complete tabulation of the data can be found in Ref. 9.

[15]B. J. C. van der Hoeven, D. T. Teaney, and V. L. Moruzzi, Phys. Rev. Letters 20, 719 (1968).

[16]G. S. Dixon and J. E. Rives, Phys. Rev. 177, 871 (1969).

[17]D. T. Teaney, Phys. Rev. Letters 14, 898 (1965).

[18]See, for example, J. Skalyo and S. A. Friedberg, Phys. Rev. Letters 13, 133 (1964).

[19]G. A. Baker, Phys. Rev. 129, 99 (1963).

[20]D. S. Gaunt and C. Domb, J. Phys. C 1, 1038 (1968).

[21]M. E. Fisher, Lectures in Theoretical Physics (University of Colorado Press, Boulder, Colo., 1965), Vol. VII C, pp. 1–159.

[22]D. T. Teaney, B. J. C. van der Hoeven, and V. L. Morruzzi, Phys. Rev. Letters 20, 722 (1968).

[23]T. Yamamoto, O. Tanimoto, Y. Yusada, and K. Okada, Natl Bur. Std. (U. S.), Misc. Publ. No. 273,

pp. 86–91.

[24]T. Nagamiya, K. Yosida, and R. Kubo, Advan. Phys. 4, 2 (1955).

[25]M. E. Fisher, Proc. Roy. Soc. (London), A254, 66 (1960).

[26]A. Bienenstock, J. Appl. Phys. 37, 1459 (1966).

Neutron and Optical Investigation of Magnons and Magnon-Magnon Interaction Effects in NiF$_2$

M. T. Hutchings* and M. F. Thorpe*

Brookhaven National Laboratory,   Upton, New York 11973

and

R. J. Birgeneau,† P. A. Fleury, and H. J. Guggenheim

Bell Telephone Laboratories, Murray Hill, New Jersey 07974

(Received 7 April 1970)

Neutron inelastic scattering and Raman light scattering have been used to investigate spin-wave excitations in the canted antiferromagnet NiF$_2$. All the zone-center Raman-active phonons have been observed as well. By neutron scattering, we have measured the dispersion of one-magnon excitations in the (010) plane of the crystal. These data have been analyzed, together with published values for the antiferromagnetic-resonance mode frequencies, to give values for the two anisotropy parameters and three exchange constants in the spin Hamiltonian for the crystal. We find $D = 4.36$ (± 0.14) cm^{-1}, $E = 1.66$ (± 0.03) cm^{-1}, J_1 (coupling ions along the c axis) $= -0.22$ (± 0.50) cm^{-1}, J_2 (coupling corner to body center ions) $= 13.87$ (± 0.36) cm^{-1}, and J_3 (coupling ions along the a or b axes) $= 0.79$ (± 0.40) cm^{-1}. From these parameters, we have calculated the density of magnon states and find that it shows one sharp peak near 108 cm^{-1}. The one-magnon Raman scattering confirms the values of the antiferromagnetic-resonance frequencies, while the second-order (two-magnon) scattering gives a broad line corresponding to a weighted two-magnon density of states centered at 203 cm^{-1}. We have interpreted the two-magnon line shape in terms of the neutron data by a Green's-function theory which includes the effect of magnon-magnon interaction. In this theory of line shape, the density of states is approximated by a one-exchange-parameter model, corresponding to a weighted zone-boundary energy. Nevertheless, excellent agreement with experiments is obtained. This study, therefore, has served to characterize completely the interactions in NiF$_2$, and, in addition, it has supplied the first detailed comparison of neutron and Raman data for an $S = 1$ ion.

I. INTRODUCTION

Nickel fluoride NiF$_2$ has the rutile crystal structure[1] and orders below 73.2 °K^2 to form a slightly canted two-sublattice antiferromagnet. Unlike the isomorphic compounds MnF$_2$, FeF$_2$, and CoF$_2$, the spins lie in the a-b plane of the crystal and are tilted away from the axes by a small angle $\sim 0.5°$.[3-5] This tilt gives rise to a small ferromagnetic moment which modifies the magnetic properties from those of a conventional antiferromagnet.[6-8]

We have investigated the magnon dispersion relations in this compound by both neutron scattering and light scattering. By inelastic neutron scattering, the dispersion may be studied throughout the Brillouin zone, since the neutron wave vector is of the same order of magnitude as that of the shortest-wavelength magnons. The data may be readily analyzed to obtain values for the anisotropy and exchange constants in the spin Hamiltonian of the crystal. Indeed, neutron scattering is perhaps the most direct method of obtaining exchange constants in an antiferromagnetic compound. In the case of NiF$_2$, it permits unambiguous determination of the values whereas other methods have previously given conflicting results.[6-10]

Raman light scattering provides information on both one- and two-magnon excitations, as well as optical phonons. However, the technique is limited to exploration of small wave-vector excitations because of the small momentum carried by the incident photons $\approx 10^{-3}$ Å^{-1}. In first-order scattering, therefore, Raman experiments provide information only on the excitations near the center of the Brillouin zone. This is true for both one-magnon and phonon excitations. However, light scattering is also sensitive to two-magnon excitations of essen-